Assessment of L5 receiver performance in presence of interference using a realistic receiver simulator

Frédéric Bastide, Christophe Macabiau, Dennis Akos, Benoit Roturier

Assessment of L5 Receiver Performance in presence of Interference using a Realistic Receiver Simulator

Frederic Bastide, ENAC/STNA, France
Christophe Macabiau, ENAC, France
Dennis Akos, Stanford University
Benoit Roturier, STNA, France

BIOGRAPHIES

Frederic Bastide graduated as an electronics engineers at the ENAC, the French university of civil aviation, in 2001, Toulouse. He is now a Ph.D student at the ENAC. His researches focus on the study of dual frequencies receivers for civil aviation use. Currently he is working on DME/TACAN signals impact on GNSS receivers. He also spent 6 months at the Stanford GPS Lab earlier this year as an exchange researcher.

Dennis M. Akos completed the Ph.D. degree in Electrical Engineering at Ohio University conducting his graduate research within the Avionics Engineering Center. After completing his graduation he has served as a faculty member with Luleå Technical University, Sweden and is currently a research associate with the GPS Laboratory at Stanford University. His research interests include GPS/CDMA receiver architectures, RF design, and software radios.

Christophe Macabiau graduated as an electronics engineer in 1992 from the ENAC (Ecole Nationale de l'Aviation Civile) in Toulouse, France. Since 1994, he has been working on the application of satellite navigation techniques to civil aviation. He received his Ph.D. in 1997 and has been in charge of the signal processing lab of the ENAC since 2000.

Benoit Roturier graduated as a CNS systems engineer from Ecole Nationale de l'Aviation Civile (ENAC), Toulouse in 1985 and obtained a PhD in Electronics from Institut National Polytechnique de Toulouse in 1995. He was successively in charge of Instrument Landing Systems at DGAC/STNA (Service Technique de la Navigation Aerienne), then of research activities on CNS systems at ENAC. He is now head of GNSS Navigation subdivision at STNA and is involved in the development of civil aviation applications based on GPS/ABAS, EGNOS and Galileo.

ABSTRACT

In the frame of the GPS modernization program, a third civil GPS signal, called L5, will be broadcasted by the first Block IIF satellites launched in 2005. The signal band is located in an ARNS band so that it is of particular interest for users such as civil aviation. It is expected to increase accuracy, availability, integrity and continuity of service.

A receiver dedicated to this signal requires special design. Signal modulation is different from that used on the L1 signal in that there are two components, in phase quadrature with each other, available to the user. The first carries data while the second, called the pilot component, does not. Different tracking configurations may be considered either combined or not. Moreover, the spectral environment in this band is different from what can be found around L1. For instance, the L5 band is expected to face a strong interference environment mainly because of pulsed DME/TACAN signals. The aim of this paper is to present a visual and realistic L5 signal generator and receiver simulator that implements various tracking schemes. In addition, a complete front-end performing digital pulse blanking is simulated. It is based on a previously validated L1 simulator and has been developed under the Labview environment. This development software enables a very visual tool with, for instance, code and phase error stresses, integrate & dump prompt samples but also ADC bins distribution are visualized in real-time. It helps to understand how the receiver behaves in various cases. This tool is used to estimate tracking performance in normal conditions of use but also in

presence of different types of interference that can be generated.

INTRODUCTION

A third civil GPS signal, called L5, will be broadcasted by the first Block IIF satellites launched in 2005 in an ARNS band. This signal has two components in phase quadrature, only one carrying data available to civil users. Signal acquisition and tracking may be performed using the two components separately or using a combined scheme. Various papers such as [Tran, 2003] have addressed the choice of the tracking configuration by carrying out simulations. The result is that tracking using only the pilot component leads to the lowest tracking thresholds. The usefulness of having a receiver simulator is obvious; all these options may be tested.

Moreover, the L5 band is expected to face a strong interference environment mainly because of pulsed DME/TACAN signals that may be disruptive if no careful design is chosen. Degradation of such interference have already been theoretically studied and presented [Hegarty, 1996]. The L5 receiver simulator was then used to estimate DME/TACAN signals impact on the receiver and compare results with theory.

The first part of the paper describes the simulator functions (e.g.: useful signal and interference generation). Then, the simulator interface itself is presented and finally, in the third part, results in presence of interference are shown.

SIMULATOR DESCRIPTION

The simulator emulates a single channel and carries out the following functions (also shown in the next figure):

- Signals generation
  - GPS L5 signal
  - Receiver thermal noise
  - Interference
- Front-end
  - Equivalent RF/IF signal filtering
  - Automatic Gain Control (AGC) and Analog to Digital Converter (ADC)
  - Digital pulse blanking
- Tracking loops
  - Phase lock loop (PLL)
  - Delay lock loop (DLL)
  - NAV bit synchronization
  - C/N_0 estimation
  - Neuman-Hoffman codes and Nav data synchronization

Each of these functions is studied in the following.

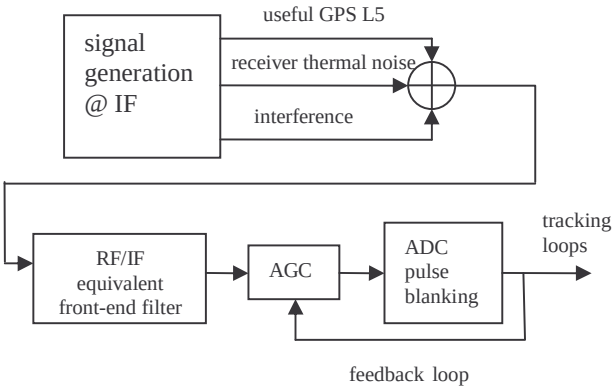

Figure 1 L5 receiver simulator diagram

L5 signal generation

The L5 signal consists of a QPSK modulation. There are so two carrier components that are in phase quadrature with each other. Each carrier component, the Inphase (I) carrier and the quadraphase carrier (Q), is BPSK modulated by a separate bit train. Bit trains are described below:

- **Inphase carrier**

The bit train is the modulo-2 sum of the I5 code, NAV data and a synchronisation sequence. The I5 code has a period of 10230 chips and is generated at 10.23 Mchips/s so that one period lasts 1 ms. A 24-bit cyclic redundant code is added to every 267 bits of the GPS L5 NAV to form a 300 bits data message frame generated at 50 bps. Then this message is convolutionally encoded with a rate ½, constraint length 7 code resulting in a 100 sps symbol stream. Finally, each symbol is synchronized with the synchronization sequence that is a 10-symbol Neuman-Hoffman code clocked at the 1 ms I5 code period. The I component carries data and is called the *data channel*.

- **Quadraphase carrier**

This bit train is not very different from the previous one, the main difference is that no data is present. More precisely, it consists of the modulo-2 sum of the Q5 code and another synchronisation sequence. The Q5 code has also a period of 10230 chips and is generated at 10.23 Mchips/s so that one period lasts 1 ms. Now, the synchronisation sequence is a 20-symbol Neuman-Hoffman code clocked at the 1 ms Q5 code period.

For a particular SV, all transmitted signal elements (carriers, codes, synchronisation sequence and data) are

coherently derived from the same on-board frequency source.

The simulated GPS L5 signal is directly generated at the intermediate frequency (IF). Aliasing occurs, but the effects are minimized by using a sufficiently high sampling frequency (typically 160 MHz for our simulations). Here is the generated digital signal expression:

$$\begin{aligned} s(k) = &\sqrt{C_{tot}}\, d(kT_s - \tau(kT_s))XI(kT_s - \tau(kT_s)) \\ &.NH_{10}(kT_s - \tau(kT_s)).\cos(2\pi f_{IF} kT_s - \theta(kT_s)) \\ &+ \sqrt{C_{tot}}\, XQ(kT_s - \tau(kT_s))NH_{20}(kT_s - \tau(kT_s)) \\ &.\sin(2\pi f_{L5} kT_s - \theta(kT_s)) \end{aligned}$$

where

- C_{tot} is the total (data+pilot) received power at the antenna output
- $d(k)$ is the navigation message
- $XI(k)$ and $XQ(k)$ are respectively the PRN codes used on data and pilot components
- $NH_{10}(k)$ and $NH_{20}(k)$ are respectively the Neuman-Hoffman codes used on data and pilot components
- τ is the propagation delay
- f_{IF} is the intermediate frequency
- T_s is the sampling period
- θ is the carrier phase

Dynamics may be included by the user such as Doppler frequency offsets or line of sight acceleration terms. Moreover, an arbitrary constant code delay or constant phase offset may be included. These parameters are used to test the behavior of code and phase tracking loops but also to simulate receiver dynamics. The acquisition process is not simulated so that the user can not directly include the real carrier Doppler frequency and code delay. Instead the user can select their estimation errors after the acquisition process. Thus the generated signal is constructed using these initial estimation errors.

In the nominal case, only Gaussian thermal noise is added to the useful GPS signal. It is characterized by its double-sided power spectral density $\frac{N_0}{2}$.

User-accessible parameters for GPS L5 signal generation are

- satellite vehicle identity
- Useful signal power before front-end filtering
- Sampling frequency
- Intermediate frequency
- Constant code offset
- Constant carrier offset
- Doppler frequency
- Doppler velocity
- Thermal noise PSD

Interference generation

Different kinds of interference may be generated in the simulator:

- **Continuous wave interference (CW)**
  Available parameters are the Jammer-to-Signal ($\frac{J}{S}$) ratio and the frequency offset Δf with respect to L5.

- **Frequency Modulation (FM) interference**
  The user can select the frequency offset with respect to L5, the ratio $\frac{J}{S}$ and the Carson band that is an empirical estimation of the FM signal bandwidth.

- **DME\TACAN pulsed signals**
  Available parameters are the number of signals, J/S, frequency offset and pulse repetition frequency (PRF)

Note: these interference are also generated at IF.

Then the useful GPS L5 signal, thermal noise and interference are added and the resulting incoming signal is filtered by the equivalent front-end filter representing a combination of RF and IF filtering in a real receiver. As a basis, we considered two different out-of-band filtering requirements at L5/E5a. The first one is proposed by RTCA, [Hegarty, 1996], and the other one by EUROCAE. Next figure shows both requirements and simulated filters.

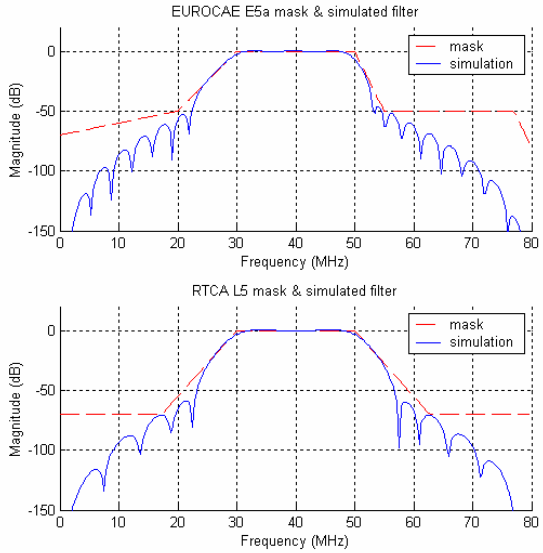

Figure 2 *RTCA and EUROCAE interference masks and simulated filters*

The equivalent filter is generated as a succession of a IIR Butterworth filter and a FIR filter. Steep slope just out of the pass-band is due to the FIR filter that simulates IF filters effects. Lower slope away from the pass-band is brought by the Butterworth filter as RF filters do in real receivers. We sought to simulate filters as close as possible to the requirements.

After filtering, the signal is quantized using a uniform non-centered quantization law. So as to decrease quantization losses, a post-ADC AGC is implemented. It is a variable gain amplifier that is driven by ADC output sample statistics and more precisely by the ADC bins distribution [Bastide, 2003]. In presence of thermal Gaussian noise only, it may be shown, [Van Dierendonck, 1996] [Chang, 1982], that the Signal-to-Noise ratio (SNR) degradation at correlator output is only a function of the ratio of the maximum quantization threshold to noise standard deviation. Next figure plots SNR degradation at correlator output for several bits in the case of a uniform non-centered quantization law. Front-end filtering and limited sampling frequency are not accounted for.

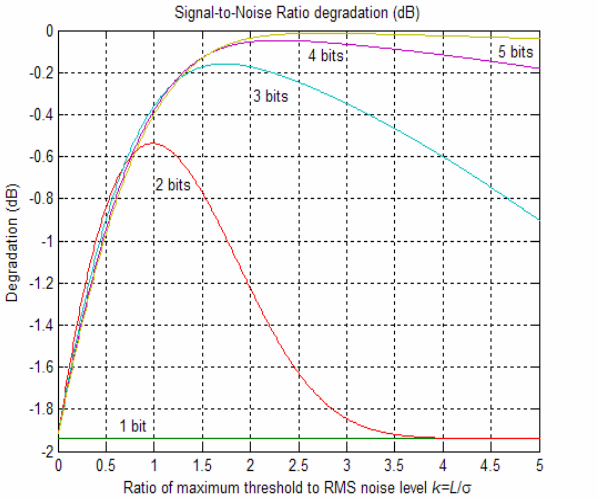

Figure 3 *SNR degradation at correlator output due to quantization. Precorrelation filtering and finite sampling frequency effects are neglected*

There is an optimal ratio that minimizes those quantization losses. The role of the AGC is to ensure this ratio is respected. The automatic gain control is implemented as a first order feedback loop. The user can select the time constant of the AGC that is generally of the order of a few milliseconds.

The digital pulse blanking principle is described in [Grabowsky, 2002] and is implemented in the simulator so as to cope with pulsed interference. This method is much simpler than analog pulse blanking first proposed in [Hegarty, 2000]. Indeed, no pulse detector circuit is required to identify the beginning and end of each pulse. Further, the implementation does not need memory to track samples that are part of a pulse. Samples are zeroed on a sample-by-sample: each quantized sample larger than a threshold is zeroed. Even if there are some disadvantages, this method is likely to be one selected in future GNSS receivers as a result of the simplicity of the design. It requires more bits than necessary in digital tracking loops. For instance, the next plot show the optimal, from Fig. 3, 3-bit ADC bins distribution represented over 4 bits. Thus, a 4-bit ADC is used in the receiver but only 3-bit samples are fed to digital tracking loops. Output quantized signal is between -15 and +15 by steps of 2.

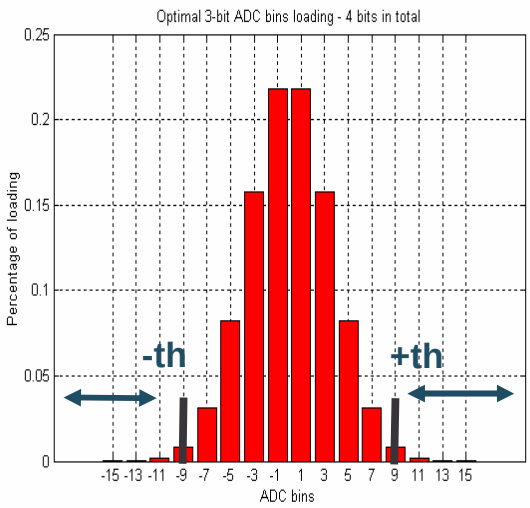

Figure 4 Optimal 3-bit loading using a 4-bit ADC

The blanking threshold th is selected on this distribution and blanked samples are set to zero. Other samples are grouped so as to get a representation on 3 bits and then fed to digital tracking loops.

User-accessible parameters for AGC/ADC systems are

- AGC time constant
- Useful bits used in digital tracking loops
- Total number of bits
- Blanking threshold

Tracking loops

One difference with the GPS L1 signal is the presence of an additional component accessible to civil users: the pilot component. This one is in phase quadrature with the data component and does not carry any data. [Hegarty, 1999] demonstrated the advantage of using both data and pilot components to increase accuracy. Code and carrier tracking error standard deviation may be reduced by implementing a linear combination of discriminators. The accuracy may be improved by the square-root of 2 at high C/N_0 when compared to the use of the pilot channel only.

However, an issue arises when it comes to carrier phase tracking. If the two same discriminators are used on each component then the combination is easy. Otherwise, assume a classical Arctangent Costas PLL is implemented on the data component and an extended Arctangent PLL on the pilot component. Because of different linear regions, this combination requires a detection of $\pm\pi$ jumps that may arise on the data component discriminator. [Macabiau, 2002] has shown that there is no advantage to perform this correction. Indeed, the C/N_0 required to perform robust jumps detections is higher than the tracking threshold using the pilot component only. Thus, there is little gain if continuous phase tracking is the objective.

Moreover, it was also demonstrated that the carrier tracking threshold is lower when carrier phase tracking is only performed on the pilot component [Tran, 2003]. The reason is that carrier tracking error is tracked at its value and not twice as it is done in the data discriminator. Indeed a pure PLL may be implemented on the pilot component.

For code tracking, there is no issue of combination since only two identical discriminators can be used. Thus, accuracy may be easily increased.

The opinion of several experts is that there is no reason to use the data channel for both code and carrier tracking. Indeed most users, such as civil aviation, only care about at which C/N_0 carrier cycle slip occurs. Moreover, even if code tracking is more accurate using both components, tracking errors due to noise are much smaller than other (e.g., multipaths) errors. The achievable improved accuracy is not worth the extra complexity.

Different tracking configurations combined or not, may be implemented in the receiver simulator. Whatever is the configuration, code tracking loop is a first order loop using either Early-Minus-Late (EML) or dot-product discriminators. For a single component, performance in Gaussian thermal noise are respectively:

$$\sigma_\tau^2 = \frac{B.d}{\frac{C_{tot}}{N_0}}\left(1+\frac{4}{T_p(2-d)\frac{C_{tot}}{N_0}}\right)(chip)^2$$

and

$$\sigma_\tau^2 = \frac{B.d}{\frac{C_{tot}}{N_0}}\left(1+\frac{2}{T_p\frac{C_{tot}}{N_0}}\right)(chip)^2$$

where

- B is the equivalent loop noise bandwidth
- C_{tot} is the total received power
- d is the Early/Late delay
- T_p is the coherent integration time of the I&D filters. The predetection bandwidth is so $f_P = \frac{1}{T_P}$

Moreover, code tracking is aided by carrier phase tracking loop. Carrier phase tracking loop is a third order loop whose loop filter is indicated in [Stephens, 1995]. Carrier discriminators on the data component are either a classical Arctangent or a Product discriminator. On the pilot component, an extended Arctangent or a normalized Q discriminator (pure PLL) is implemented. Using the data component, carrier phase tracking error variance is

$$\sigma_\theta^2 = \frac{2B}{\frac{C_{tot}}{N_0}}\left(1+\frac{1}{T_p\frac{C_{tot}}{N_0}}\right)\ (rd)^2$$

If only the pilot component is used, squaring losses are suppressed so the tracking error variance is

$$\sigma_\theta^2 = \frac{2B}{\frac{C_{tot}}{N_0}}\ (rd)^2$$

Data bits estimation

Data bits are simply estimated from the sign of the prompt Inphase correlator on the data component.

Signal-to-noise density ratio estimation

The C/N_0 is estimated at correlator output according to the following equation

$$\frac{\hat{C}}{N_0} = \frac{E\left(I_{P,pilot}\right)^2}{\mathrm{var}\left(I_{P,pilot}\right)}\cdot f_p$$

where $I_{P,pilot}$ is the prompt correlator output sample on the pilot component.

Neuman-Hoffman codes/Nav data synchronization

Neuman-Hoffman code synchronization is equivalent to data bit synchronization since the two trains are synchronized. A very convenient and robust way to do it is to form the NH20 autocorrelation function, see next figure, on the prompt pilot component. More precisely, pilot prompt samples are cross-correlated with a stored NH20 sequence whose delay takes all the twenty possible values. The estimated offset corresponds to the maximum of this cross-correlation function. Once this synchronization is performed, coherent integration up to 10 ms is possible on the data component. Of course, larger integrations are possible on the pilot component.

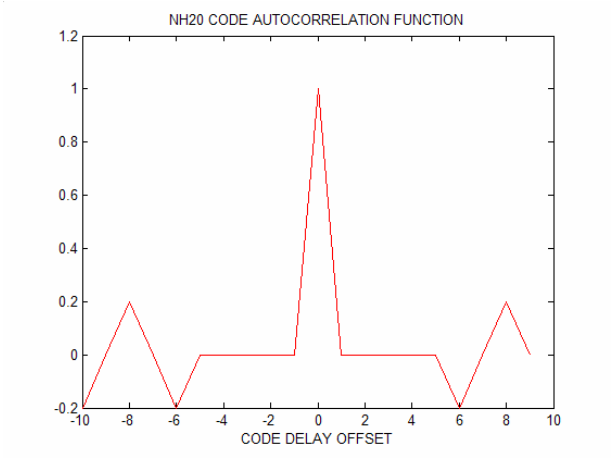

Figure 5 NH20 code autocorrelation function

Generic L5 receiver architecture

Next plot shows the generic simulator tracking loops diagram.

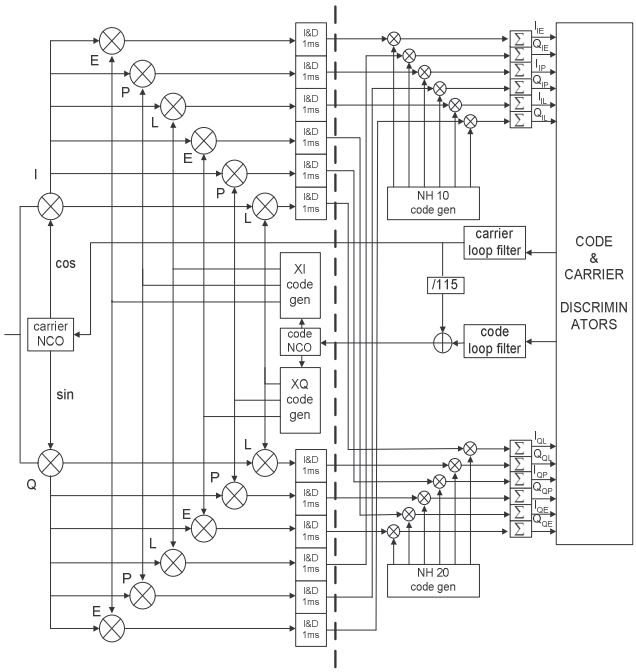

Figure 6 L5 receiver simulator tracking loops diagram

The number of correlators may be reduced if code and phase tracking is only performed using the pilot component. Indeed, Early and Late I's and Q's but also the Q prompt correlator may be suppressed on the data component. The indicated diagram is voluntary general.

Correlator output samples are expressed below in presence of thermal noise only. For the data component,

$$
\begin{cases}
I_{IE}(k) = \sqrt{\frac{C_{tot}}{4}} d(k) NH_{10}(k) \frac{\sin(\pi \Delta f T_P)}{\pi \Delta f T_P} R_{XI}\left(\varepsilon_\tau + \frac{d}{2}\right) \cos(\varepsilon_\theta) + n_{I_{IE}}(k) \\
I_{IP}(k) = \sqrt{\frac{C_{tot}}{4}} d(k) NH_{10}(k) \frac{\sin(\pi \Delta f T_P)}{\pi \Delta f T_P} R_{XI}(\varepsilon_\tau) \cos(\varepsilon_\theta) + n_{I_{IP}}(k) \\
I_{IL}(k) = \sqrt{\frac{C_{tot}}{4}} d(k) NH_{10}(k) \frac{\sin(\pi \Delta f T_P)}{\pi \Delta f T_P} R_{XI}\left(\varepsilon_\tau - \frac{d}{2}\right) \cos(\varepsilon_\theta) + n_{I_{IL}}(k) \\
Q_{IE}(k) = \sqrt{\frac{C_{tot}}{4}} d(k) NH_{10}(k) \frac{\sin(\pi \Delta f T_P)}{\pi \Delta f T_P} R_{XI}\left(\varepsilon_\tau + \frac{d}{2}\right) \sin(\varepsilon_\theta) + n_{Q_{IE}}(k) \\
Q_{IP}(k) = \sqrt{\frac{C_{tot}}{4}} d(k) NH_{10}(k) \frac{\sin(\pi \Delta f T_P)}{\pi \Delta f T_P} R_{XI}(\varepsilon_\tau) \sin(\varepsilon_\theta) + n_{Q_{IP}}(k) \\
Q_{IL}(k) = \sqrt{\frac{C_{tot}}{4}} d(k) \frac{\sin(\pi \Delta f T_P)}{\pi \Delta f T_P} R_{XI}\left(\varepsilon_\tau - \frac{d}{2}\right) \sin(\varepsilon_\theta) + n_{Q_{IL}}(k)
\end{cases}
$$

And for the pilot component,

$$
\begin{cases}
I_{QE}(k) = -\sqrt{\frac{C_{tot}}{4}} NH_{20}(k) \frac{\sin(\pi \Delta f T_P)}{\pi \Delta f T_P} R_{XQ}\left(\varepsilon_\tau + \frac{d}{2}\right) \sin(\varepsilon_\theta) + n_{I_{QE}}(k) \\
I_{QP}(k) = -\sqrt{\frac{C_{tot}}{4}} NH_{20}(k) \frac{\sin(\pi \Delta f T_P)}{\pi \Delta f T_P} R_{XQ}(\varepsilon_\tau) \sin(\varepsilon_\theta) + n_{I_{QP}}(k) \\
I_{QL}(k) = -\sqrt{\frac{C_{tot}}{4}} NH_{20}(k) \frac{\sin(\pi \Delta f T_P)}{\pi \Delta f T_P} R_{XQ}\left(\varepsilon_\tau - \frac{d}{2}\right) \sin(\varepsilon_\theta) + n_{I_{QL}}(k) \\
Q_{QE}(k) = \sqrt{\frac{C_{tot}}{4}} NH_{20}(k) \frac{\sin(\pi \Delta f T_P)}{\pi \Delta f T_P} R_{XQ}\left(\varepsilon_\tau + \frac{d}{2}\right) \cos(\varepsilon_\theta) + n_{I_{QE}}(k) \\
Q_{QP}(k) = \sqrt{\frac{C_{tot}}{4}} NH_{20}(k) \frac{\sin(\pi \Delta f T_P)}{\pi \Delta f T_P} R_{XQ}(\varepsilon_\tau) \cos(\varepsilon_\theta) + n_{I_{QP}}(k) \\
Q_{QL}(k) = \sqrt{\frac{C_{tot}}{4}} \frac{\sin(\pi \Delta f T_P)}{\pi \Delta f T_P} R_{XQ}\left(\varepsilon_\tau - \frac{d}{2}\right) \cos(\varepsilon_\theta) + n_{I_{QL}}(k)
\end{cases}
$$

where

- Δf is the carrier frequency tracking error
- R_{XI} and R_{XQ} are, respectively, the data and the pilot PRN codes autocorrelations
- ε_τ is the code tracking error
- ε_θ is the phase tracking error equal, to first order, to $\varepsilon_\theta = 2\pi \Delta f T_P + \Delta\theta_0$, where $\Delta\theta_0$ is a constant phase tracking error

The last terms in each equation are the noise components.

So as to validate our receiver tracking loops implementation, some tests were carried out. Chosen equivalent loops noise bandwidths are respectively 10 Hz and 1.5 Hz for the carrier and code tracking loops. Predetection integration time is 10 ms, there is no quantization and front-end filter effects can be neglected. The real code and carrier tracking errors are stored and variances are computed for various Signal-to-Noise density ratios (C/N_0). Obtained results are compared to theoretical expressions. Tracking is performed on the pilot component only.

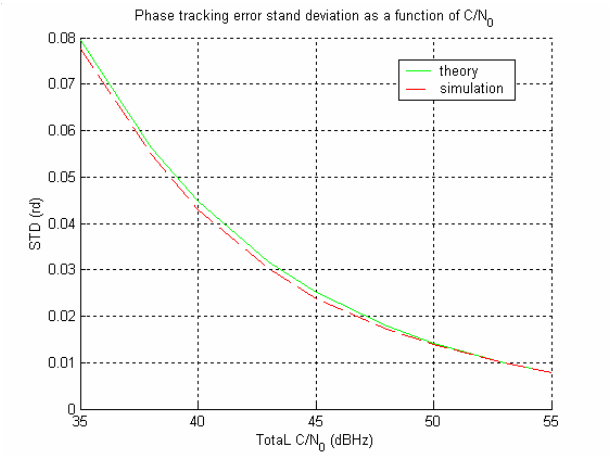

Figure 7 Theoretical and simulated phase carrier tracking error standard deviation as a function of the total (I+Q) C/N_0

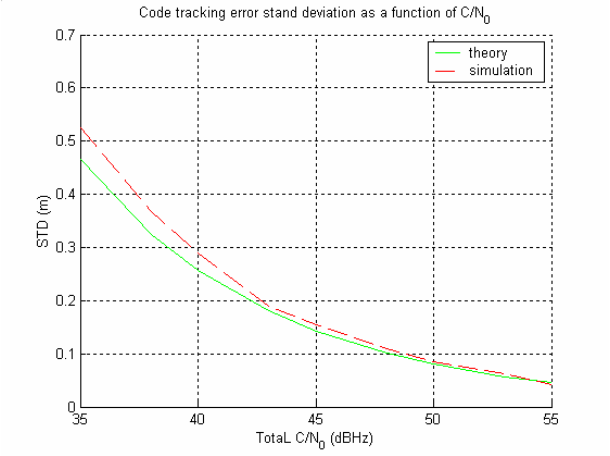

Figure 8 Theoretical and simulated code carrier tracking error standard deviation as a function of the total (I+Q) C/N_0

The results obtained are very close to theory, validating our tracking loops implementation.

User-accessible parameters for tracking processes are

- Combined tracking or not
- Carrier phase tracking
  - Classical Arctangent, Product, Pure PLL or extended arctangent discriminators
  - Loop equivalent noise bandwidth
- Code tracking
  - EML or Dot-Product discriminators

- Loop equivalent noise bandwidth
- E/L spacing

EXAMPLE OF SIMULATOR INTERFACE

Here is an example of the simulator interface in the case of the nominal tracking configuration (use of the pilot component only: pure PLL and EML code discriminator) and when only DME/TACAN signals are generated.

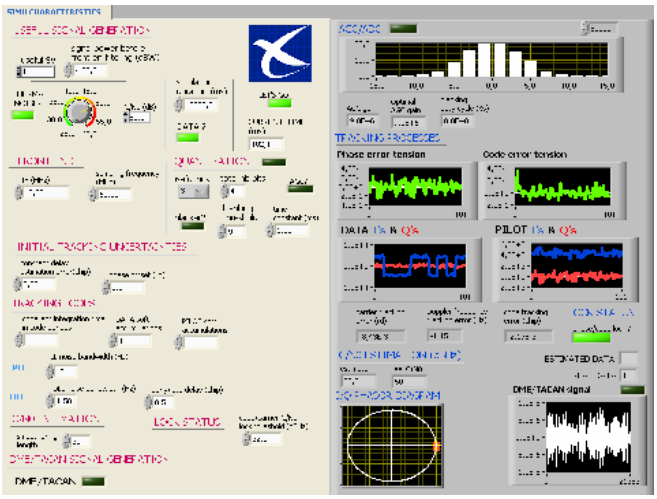

Figure 9 L5 receiver simulator interface in the nominal tracking configuration

On the left hand side panel all the user parameters are available whereas on the right hand side part, simulation results are displayed in real time. From the top to the bottom, the results are:

- ADC bins distribution plot, blanking duty cycle and AGC gain
- DLL,PLL error tensions
- Data and pilot I's and Q's
- Real instantaneous code, carrier and frequency tracking errors
- C/N_0 estimate
- Current data, NH10 and NH20 bits value. Data estimate is also indicated
- I/Q phasor diagram for both data and pilot components. Each point is located on the unity circle and has for coordinates:
  - the x-axis is the normalized I prompt sample
  - y-axis is the normalized Q prompt sample

  Thus carrier tracking error evolution is directly observable
- simulated DME/TACAN signals

INTERFERENCE TESTS RESULTS

Since DME/TACAN signals impact on L5 receiver performance is a primary issue, we focused on this type of interference.

DME/TACAN signals generation

The L5 band interference environment is presented in [Hegarty, 1996]. It is highlighted that the major existing systems in the L5 band are pulsed and that the primary threat is DME/TACAN signals. These are pulse-ranging navigation systems operating in the 960-1215 MHz frequency band. DME signal provides distance measurement between the aircraft and a ground station. TACAN also provides azimuth information and is a military system. This navigation system consists of an airborne interrogator and a ground-based transponder. DME/TACAN operate in four modes (X, Y, W and Z) and only the X-mode replies in the 1151-1213 MHz frequency band. X-mode replies are made of pulse pairs with an inter-pulse interval of 12 µs. Ground stations transmit pairs at a maximum rate (pulse repetition frequency- PRF) of 2700 for DME and 3600 for TACAN. Each pulse has a 3.5 µs half-amplitude and a pair may be modeled using the following formula [Monnerat, 2001]:

$$s_{DME}(t) = e^{\frac{-\alpha t^2}{2}} + e^{\frac{-\alpha (t-\Delta t)^2}{2}}$$

where

- α =4.5e11 s^{-2}
- Δt =12e-6

Thus DME and TACAN signals transmitted by a ground station are well approximated as a succession, of Gaussian-shape pulse pairs modulating a carrier, [Tran, 2001]. Arrival times of pair pulses may be assumed independent and of constant behavior over time. Thus a convenient modelization of arrival times of each pair is a Poisson distribution with parameter λ equal to the PRF. An illustration of such DME/TACAN signal generation is given on the next plot over 2 ms and for a sampling frequency of 160 MHz:

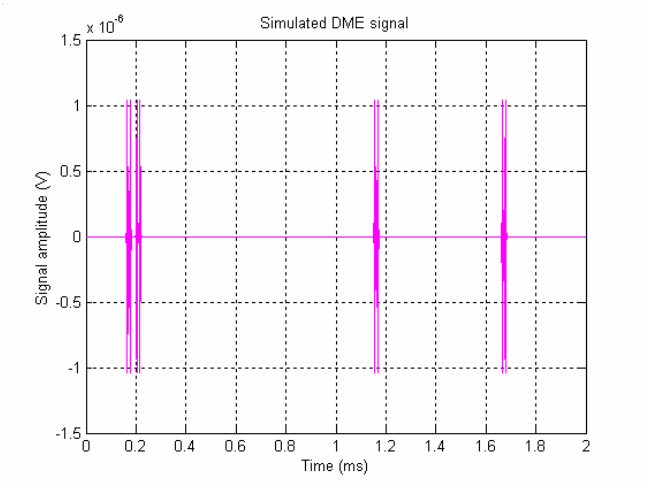

Figure 10 Simulated DME signal over 2 ms

Here is a close-up of the first generated pair:

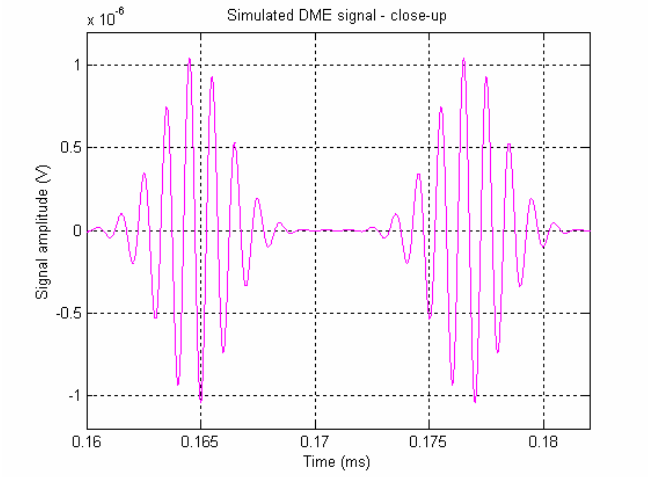

Figure 11 Close-up on the first generated pulse pair

Using this methodology to generate DME/TACAN signals, pulse pairs collision occurs. Next is a plot of the simulated DME/TACAN signals over a specific location in Europe:

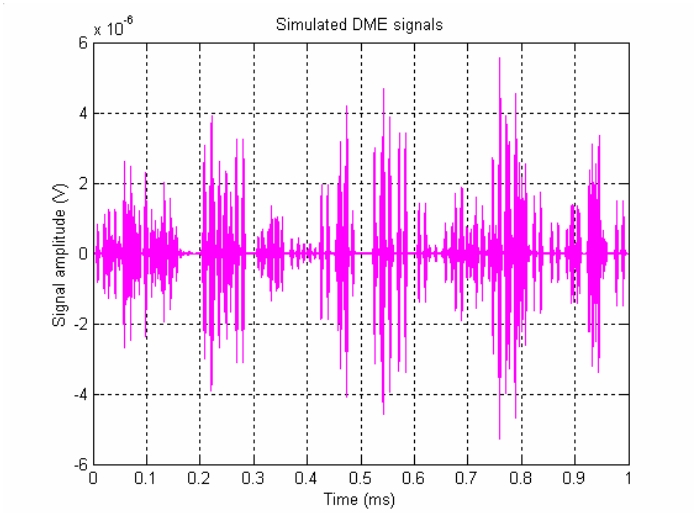

Figure 12 Composite generated DME/TACAN signals at the antenna output of a GNSS receiver over Europe

Here is a close-up illustrating pulse pair collision

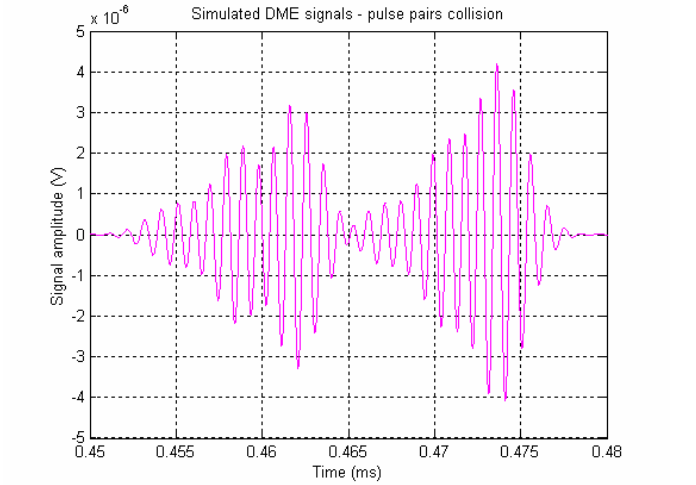

Figure 13 Example of pulse pairs collision

Two methodologies that do not take into account pulse pairs collisions have been published. The first one was initially used by RTCA to assess DME/TACAN signals impact on GPS L5 receivers, [Hegarty, 1996]. The focus here is on the second methodology indicated in [Monnerat, 2001]. Pulses collisions are not considered in both theories; it is a conservative assumption since they undoubtedly do occur. Signal-to-Noise density ratio degradation is given by the following equation:

$$\deg\left(\frac{C}{N_0}\right)=\frac{1-Bdc+\frac{1}{N_0}\sum_{1}^{N}2.P_i.PW.PRF_i.C_I(\Delta f_i)}{(1-Bdc)^2}$$

where

- Bdc is the blanker duty cycle, it corresponds to the blanker activation time by unity of time
- N is the total number of low pulses whose peak power is below the blanking threshold
- P_i is the peak received power of the i-th undesired signal
- PW is the pulse width. For DME/TACAN, it is defined by half-voltage:

$$PW=\frac{1}{P_i}\int_{-\infty}^{+\infty}p(t).dt=2.6\,\mu s$$

- PRF_i is the pulse repetition frequency of the i-th low level DME/TACAN signal
- $C_I(\Delta f_i)$ is the interference coefficient of the i-th DME/TACAN signal at the frequency offset Δf_i.

The denominator of previous expression corresponds to the lost useful signal power due to the blanker while the numerator reflects the adjustment of noise floor due to:

- Thermal noise suppression by the blanker: $1-Bdc$
- Noise floor contribution due to low-level pulses expressed in the last term

According to results presented in [Tran, 2003] a pure PLL with an equivalent noise bandwidth of 10 Hz and an update rate of 10 ms was implemented for the tests. Code tracking is performed by an EML power DLL with a chip spacing of 0.5 chip.

A set of DME/TACAN signals was selected and simulations were run on it. Theory was also applied; results are presented in the next tables. First table corresponds to the simulated filter from the EUROCAE interference mask whereas the second table gives results for the RTCA simulated filter.

Blanking threshold (dBW)	Blanker duty cycle simu/theory	C/N0 degradation (dB) simu/theory
-118	0.18/0.37	-5.51/-5.91
-116	0.08/0.15	-5.68/-6.02

Table 1 *Simulation and theoretical results for the selected set of DME/TACAN signals using the EUROCAE simulated filter*

Blanking threshold (dBW)	Blanker duty cycle simu/theory	C/N0 degradation (dB) simu/theory
-118	0.17/0.37	-5.48/-5.86
-116	0.08/0.14	-5.71/-5.99

Table 2 *Simulation and theoretical results for the selected set of DME/TACAN signals using the RTCA simulated filter*

It is clear that the theoretical blanker duty cycle is larger (ratio of two) than the one indicated by simulation. The explanation is the conservative assumption that no pulse collisions occur. Moreover degradations estimated by theory are well approximated by the simulation results. Thus it implies that noise floor contribution due to DME/TACAN signals going through the blanker is not well modeled by the proposed theory.

CONCLUSION

The developed L5 receiver simulator turned out to be very useful in assessing degradations bought by interference. It highlighted the need to rethink previous C/N_0 degradation formula in a more realistic way to take into account pulse collisions.

References

[Van Dierendonck, 1996] A.J. Van Dierendonck, "GPS receivers", Global Positioning System: Theory and Application, B.Parkinson and J.J Spilker, JR., Ed ., Washington, D.C.: AIAA, Inc., 1996

[Chang, 1982] H.Chang, "Presmapling, Filtering, Sampling and Quantization Effects on the Digital Matched Filter Performance", *Proceedings of the International Telemetering Conference, 1982, pp. 889-915*

[Tran, 2003] M.Tran, C.Hegarty**,** "Performance Evaluations of the New GPS L5 and L2 Civil (L2C) Signals", *Proceedings of the Institute of Navigation National Technical meeting, Anaheim, CA, January 2003*

[Hegarty, 1996], Hegarty, C., T. Kim, S. Ericson, P. Reddan, T. Morrissey, and A.J. Van Dierendonck, "Methodology for Determining Compatibility of GPS L5 with Existing Systems and Preliminary Results," *Proceeding of The Institute of Navigation Annual Meeting, Cambridge, MA, June 1999.*

[Hegarty, 2000] Hegary, C., A.J. Van Dierendonck, D. Bobyn, M. Tran, T. Kim, J. Grabowski, "Suppressing of Pulsed Interference through Blanking." *Proceedings of the IAIN World Congress, San Diego, CA, June 2000*.

[Grabowsky, 2002] Grabowski, J, Hegarty, C, "Characterization of L5 Receiver Performance Using Digital Pulse blanking", *Proceeding of The Institute of Navigation GPS Meeting, Portland, OR, September 2002*.

[Monnerat, 2001] Monnerat, M, Lobert, B, Journo, S, Bourga, C, "Innovative GNSS2 navigation Signal", *Proceeding of The Institute of Navigation GPS Meeting, September 2001*

[Stephens, 1995] Stephens, S.A., and J.C. Thomas, "Controlled-Root Formulation for Digital Phase-Locked Loops," *IEEE Transactions on Aerospace and Electronic Systems*, January 1995.

[Tran, 2001] M.Tran and al., "Validation of the feasibility of coexistence of the new civil GPS signal (L5) with existing systems", MITRE paper, February 2001